Journal of Photochemistry & Photobiology A: Chemistry 387 (2020) 112153

Contents lists available at ScienceDirect

Journal of Photochemistry & Photobiology A: Chemistry

journal homepage: www.elsevier.com/locate/jphotochem

Novel fluorescent probes for L-cysteine based on the xanthone skeleton

Aleksandra Grzelakowska[a,*], Jolanta Kolińska[a,*], Małgorzata Zakłos-Szyda[b], Jolanta Sokołowska[a]

[a] Institute of Polymer and Dye Technology, Faculty of Chemistry, Lodz University of Technology, Stefanowskiego 12/16, Lodz, 90-924, Poland
[b] Institute of Technical Biochemistry, Faculty of Biotechnology and Food Sciences, Lodz University of Technology, Stefanowskiego 4/10, Lodz, 90-924, Poland

ARTICLE INFO

Keywords:
Fluorescent probes
Turn on
L-cysteine
Thiols
Xanthone

ABSTRACT

Two novel derivatives of xanthone (9*H*-xanthen-9-one, dibenzo-γ-pyrone) containing a maleimide moiety have been synthesized. Their properties were characterized by the combination of NMR, MS, electronic absorption and fluorescence spectroscopy. The reactivity of these compounds toward L-Cys as well other analytes was determined. The results show that the novel derivatives of xanthone demonstrate a high "turn-on" fluorescence response and selectivity toward L-cysteine and have the potential to act as probes to L-cysteine under physiological conditions. Reaction of 2-maleimidoxanthone (**4a)** and 2,7-dimaleimidoxanthone (**4b)** with L-Cys lead to the formation of the fluorescent products. In the presence of L-Cys, the fluorescence intensities of probes **4a** and **4b** have greatly enhanced 25-fold and 60-fold, respectively. Finally, the probes **4a**-**4b** were used to detection of thiols in the human cell line HeLa.

1. Introduction

Thiols are important molecules in intracellular milieu and in biological processes. Cysteine (Cys), homocysteine (Hcy) and glutathione (GSH) significantly affect many cellular functions. For example, GSH is one of the major endogenous antioxidants and is capable of preventing cellular component damage caused by reactive oxygen species. The ratio of GSH (reduced) and its disulfide, GSSG (oxidized), contributes to the redox potential of the cell and redox homeostasis [1,2]. Cysteine plays crucial role in the protein synthesis, detoxification, and metabolic processes [3]. Moreover, the altered levels of the thiols have been linked with several human diseases and consequences of diseases [4]. For these reasons, the detection of thiol biomolecules is vital. Fluorescent probes have emerged as a versatile tool for the detection of thiols. Because of the high sensitivity of fluorescent methods, fluorogenic probes for thiols became important tools in the studies on these analytes. The number of fluorogenic probes designed and synthesized for the detection of thiols is relatively large [5–13]. The mechanisms of action of these probes are based on various thiols-triggered reactions including nucleophilic addition [14], nucleophilic substitution [15,16], cyclisation with an aldehyde [17,18], a cleavage reaction by thiols [19,20], and other reactions [21–25]. An ideal fluorescent probe should possess some outstanding properties, such as high sensitivity and selectivity, short response time and proper optical properties [26].

N-substituted maleimides have been widely used in biological fields as thiol reagents. They react quite selectively with thiols *via* addition reactions involving their double bond. In most cases, they do not exhibit fluorescence, but the strong fluorescence is characterized of their thiol adduct products [27–30].

In this study, the xanthone was selected as the fluorophore due to its desirable photophysical properties, such as fluorescence with the maximum located in the visible region of the spectrum, high fluorescence quantum yield and large Stokes shift. The xanthones are a class of oxygen containing compounds with a broad range of biological activities such as anti-malarial, anti-tumor [31], anti-cancer [32], anti-bacterial [33], anti-oxidant [34,35] and anti-inflammatory [36]. Xanthones are also considered as inhibitors of different enzymes [37–45]. The main objectives of 9*H*-xanthen-9-ones synthesis are not only the development of more complex and varied bioactive compounds and structure-activity relationship studies [46]. Because of their excellent photochemical properties, derivatives of xanthone are used as fluorescent dyes and probes [47–49]. Some of them can be applied in electroluminescent devices [50] and as optical probes for metal ions [51], reactive oxygen species [52] or the RNA and DNA structure [53,54]. They are widely seen in a number of natural products [55,56]. Synthetic and naturally occurring xanthone derivatives exhibit diverse biological activities, which depend on the various substituents and their positions. The modifications of natural xanthone derivatives are aimed at expanding the range of their application [57,58].

The current study is a continuation of the authors' research into probes and chemosensors for the detection of biothiols [17,59–62]. In the present investigation, novel derivatives of xanthone were

* Corresponding authors.
E-mail addresses: aleksandra.grzelakowska@p.lodz.pl (A. Grzelakowska), jolanta.kolinska@p.lodz.pl (J. Kolińska).

https://doi.org/10.1016/j.jphotochem.2019.112153
Received 26 June 2019; Received in revised form 14 September 2019; Accepted 8 October 2019
Available online 13 October 2019
1010-6030/

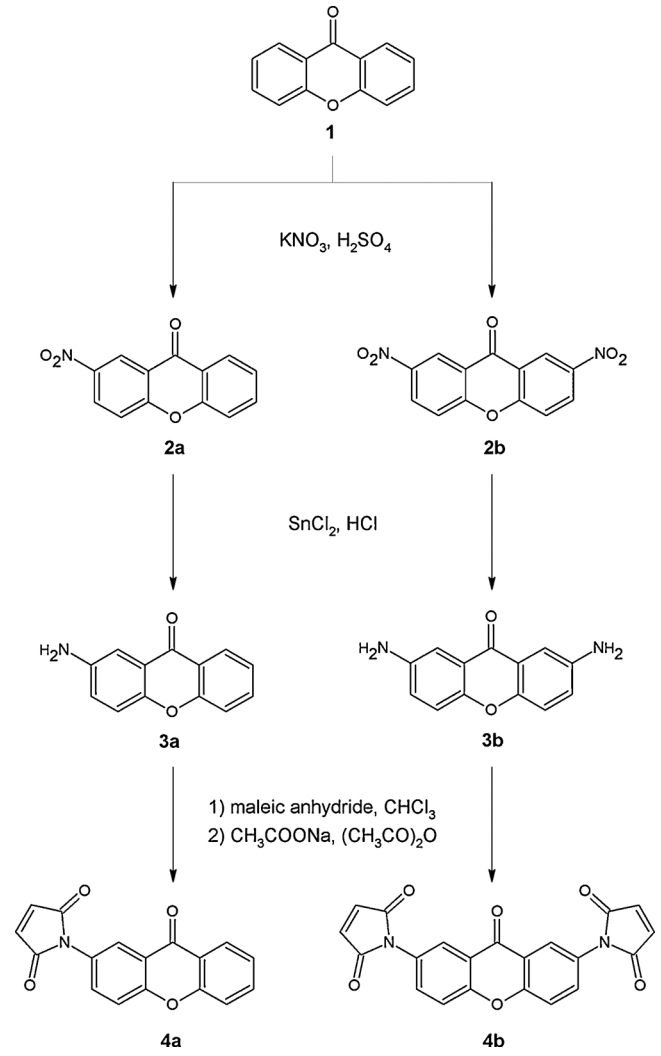

Scheme 1. Synthetic pathway used to obtain novel fluorescent probes based on a xanthone skeleton (**4a-4b**).

synthesized. The intention was to evaluate the spectroscopic properties and the study on the reactivity of novel xanthone-based probes toward L-Cys and other amino acids. These probes contain a maleimide moiety in the structures that should act as a Michael acceptor. The structures and route for the synthesis of the studied compounds: 2-maleimidoxanthone (**4a)** and 2,7-dimaleimidoxanthone (**4b)**, are shown in Scheme 1.

2. Experimental

2.1. Materials

Unless otherwise noted, all chemicals were used as received from commercial sources without further purification (Sigma-Aldrich, Poland).

2.2. Synthesis and characterization of probes

2-nitroxanthone (**2a**), 2,7-dinitroxanthone (**2b**), 2-aminoxanthone (**3a**) and 2,7-diaminoxanthone (**3b**) were synthesized according to the procedures described in the literature with minor modifications [54]. Synthesized compounds **3a**-**3b** and **4a**-**4b** were purified by column chromatography. The purity of probes **4a**-**4b** was verified using thin-layer chromatography (TLC) and was checked by high-performance liquid chromatography (HPLC). Column chromatography purifications were performed on Silica gel 60 (0.063-0.200 mm) from Merck. TLC was carried out on Merck TLC Silica gel 60 F_{254} aluminum sheets. The spots were visualized by illumination with a UV lamp (λ = 254/365 nm). HPLC analyses were performed on a Shimadzu instrument equipped with a diode array detector (DAD, SPD-M20A). The compounds were loaded onto Kinetex C18 column (Phenomenex, 100 mm × 4.6 mm, 2.6 µm) equilibrated with 10% acetonitrile in water, containing 0.1% trifluoroacetic acid. The products were eluted by an increase of the acetonitrile concentration from 10 to 100% over 10 min. The flow was kept at 1.5 mL/min. The probes were detected by monitoring absorbance at 350 nm.

The synthesized compounds were identified and characterized by proton nuclear magnetic resonance spectra (^{1}H NMR), atmospheric pressure chemical ionisation mass spectra (APCI MS), and by their melting point. NMR spectra were recorded with a Bruker Avance DPX 250 spectrometer. Solutions were prepared in $CDCl_3$, acetone-d_6 or DMSO-d_6 as a solvent, using tetramethylsilane (TMS) as internal standard. Chemical shifts (δ) are reported in parts per million (ppm), and coupling constant (J) values in hertz (Hz). NMR peak multiplicities are described as follows: s – singlet, d – doublet, dd – doublet of doublets and m – multiplets. High-resolution mass spectra were obtained with a Finnigan MAT 95 (Thermo Fisher Scientific, USA) apparatus equipped with an atmospheric-pressure chemical ionisation method. Melting points were determined on Boeöthius melting point apparatus – PGH Rundfunk, Fernsehen Niederdorf KR, Sollberg/E and uncorrected.

2a: yield: 1.40 g (29%), m.p. 199–200 °C (200–204 °C [63]), R_f 0.75 [toluene/ethanol 3:1 (v/v)].

2b: yield: 1.29 g (58%), m.p. 264–265 °C (262–265 °C [63]), R_f 0.69 [toluene/ethanol 3:1 (v/v)].

3a: yield: 0.28 g (46%), m.p. 209–211 °C (210–212 °C [64]), R_f 0.56 [toluene/ethanol 3:1 (v/v)]. ^{1}H NMR (250 MHz, $CDCl_3$): δ 8.26 (dd, J_1 = 8.0 Hz, J_2 = 1.7 Hz, 1 H), 7.67-7.59 (m, 1 H), 7.48 (d, J = 2.8 Hz, 1 H), 7.40 (d, J = 8.4 Hz, 1 H), 7.33-7.22 (m, 2 H), 7.05 (dd, J_1 = 8.9 Hz, J_2 = 2.9 Hz, 1 H), 3.78 (bs, 2 H).

3b: yield: 0.34 g (35%), m.p. 272–274 °C (269–271 °C [54]), R_f 0.47 [toluene/ethanol 3:1 (v/v)]. ^{1}H NMR (250 MHz, DMSO-d_6): δ 7.22 (d, J = 8.9 Hz, 2 H), 7.12 (d, J = 2.8 Hz, 2 H), 6.98 (dd, J_1 = 8.9 Hz, J_2 = 2.9 Hz, 2 H), 5.23 (s, 4 H).

2.2.1. Synthesis of 2-maleimidoxanthone (4a)

2-aminoxanthone **3a** (0.21 g, 1 mmol) and maleic anhydride (0.15 g, 1.5 mmol) were refluxed in chloroform (15 mL) until the disappearance of **3a**. The progress of the reaction was monitored by TLC [Merck silica gel 60, solvent acetonitrile/dichloromethane 1:1 (v/v)]. After 2 h, the resulting pale precipitate was filtered, washed with chloroform (2 × 10 mL), and dried. Acetic anhydride (10 mL) and sodium acetate (0.041 g, 0.5 mmol) were added to the obtained solid (0.28 g), and the mixture was further heated at 100 °C for 4 h. After this time the reaction mixture was concentrated under vacuum and the precipitate was filtered, washed with water (25 mL), and dried on the air. The crude product was purified by column chromatography [acetonitrile/dichloromethane 1:1 (v/v)] and crystallization from acetone. Yield: 0.15 g (52%), m.p. 175 °C, R_f 0.63 [toluene/ethanol 3:1 (v/v)]. HPLC: 99.7% purity, t_r = 5.55 min. ^{1}H NMR (250 MHz, acetone-d_6): δ 8.24 (dd, J_1 = 6.6 Hz, J_2 = 2.1 Hz, 2 H), 7.91-7.81 (m, 2 H), 7.72 (d, J = 9.0 Hz, 1 H), 7.63 (d, J = 8.5 Hz, 1 H), 7.52-7.42 (m, 1 H), 7.08 (s, 2 H). HR-APCI-MS: calculated for ($[M+H)^+$] 292.0610, found 292.0622.

2.2.2. Synthesis of 2,7-dimaleimidoxanthone (4b)

2,7-diaminoxanthone **3b** (0.23 g, 1 mmol) and maleic anhydride (0.30 g, 3 mmol) were refluxed in chloroform (20 mL) until the disappearance of **3b**. The progress of the reaction was monitored by TLC [Merck silica gel 60, solvent acetonitrile/dichloromethane 1:1 (v/v)]. After 5 h, the resulting pale precipitate was filtered, washed with

chloroform (2 × 10 mL), and dried. Acetic anhydride (15 mL) and sodium acetate (0.062 g, 0.75 mmol) were added to the obtained solid (0.36 g), and the mixture was further heated at 100 °C for 6 h. After this time the reaction mixture was concentrated under vacuum and the precipitate was filtered, washed with water (25 mL), and dried on the air. The crude product was purified by column chromatography [acetonitrile/dichloromethane 1:1 (v/v)] and crystallization from acetone. Yield: 0.28 g (72%), m.p. 211 °C, R_f 0.58 [toluene/ethanol 3:1 (v/v)]. HPLC: 99.8% purity, t_r = 5.18 min. ^{1}H NMR (250 MHz, DMSO-d_6): δ 8.69 (d, J = 2.5 Hz, 2 H), 8.35 (dd, J_1 = 9.0 Hz, J_2 = 2.5 Hz, 2 H), 8.25 (d, J = 9.0 Hz, 2 H), 7.61 (s, 4 H). HR-APCI-MS: calculated for [(M + H)$^+$] 387.0617, found 387.0619.

2.3. Spectroscopic measurements

Jasco V–670 UV–vis/NIR spectrophotometer (Jasco, Japan) was used to record steady-state absorption spectra and FLS-920 spectrofluorimeter (Edinburgh Instruments, UK) to measure steady-state emission spectra and fluorescence lifetimes [65,66]. Spectroscopic measurements were performed in a standard rectangular quartz cell (10 mm × 10 mm, 3.5 mL). To record an emission spectrum, the excitation wavelength of the absorption maximum was used (emission/excitation slit = 1nm).

Fluorescence quantum yields were determined by relative method using fluorescein reference as previously described [17].

2.4. General procedure for preparation of probes test solutions

The stock solutions of tested compounds **4a-4b** (1 mM) were prepared in acetonitrile (MeCN). The stock solutions of amino acids (L-Cys, L-Hcy, L-ACC, L-GSH, Gly, L-Glu, L-Lys, L-Met – 3 mM, L-Tyr – 2 mM), 2-mercaptoethanol (ME, 3 mM), thioglycolic acid (TGA, 3 mM), sodium bisulphite ($NaHSO_3$, 3 mM), sodium hydrosulphide (NaSH, 3 mM), sodium sulfide (Na_2S, 3 mM), hydrogen peroxide (H_2O_2, 3 mM) and N-ethylmaleimide (30 mM) were prepared in distilled water. All of the solutions were prepared immediately before the experiments. Typically, the probes (20 μM) were incubated with an appropriate amount of a stock solution of each analyte in a phosphate buffer (0.1 M, pH 7.4) at room temperature (25 °C) for 15 min. MeCN was used as a cosolvent (2%, v/v).

In these studies, an acetate buffer (0.1 M, pH 3.2–5.1), phosphate buffer (0.1 M, pH 6.4–7.8) and carbonate-bicarbonate buffer (0.1 M, pH 9.4–10.4) were used. All of the pH measurements were made with a CPI-551 microcomputer pH/ion meter (Elmetron, Poland). Each of the experiments was performed in triplicate.

2.5. Determination of cell viability and studies of the response to thiols in living cells

The human cell line HeLa was obtained from CBMM PAN Lodz. The cell line was cultured in RPMI 1640 medium (Gibco) with 10% fetal bovine serum (Gibco) supplemented with penicillin and streptomycin antibiotic at 37 °C in 5% CO_2 air atmosphere/95% air atmosphere. The HeLa cells were seeded in 96-well plates at a concentration of 1 × 10^4 cells per well. The stock solutions of the probes **4a-4b** (625 μM) were prepared in DMSO.

The cytotoxicity of the compounds **4a-4b** was determined using an MTT-based assay according to the procedure described in Ref. [67]. The cells were treated with the indicated concentrations (0–25 μM) of compounds **4a-4b** for 24 h.

To determine the response to thiols in living cells, the fluorescence intensity was measured using a Synergy 2 microplate reader (BioTek, Winooski, VT, USA) operated by the Gen5 program. For the control experiment, cells in part of wells were pretreated with 400 μM of N-ethylmaleimide and incubated at 37 °C for 20 min. A stock solution of NEM (10 mM) was prepared in distilled water. Then the HeLa cells were treated with 0–25 μM compounds **4a-4b** and were incubated for 20 min. at 37 °C. Subsequently, the fluorescence intensity at 460/40 nm was measured (λ_{ex} = 360/40 nm).

The results are expressed as optical density ratio of the treatment to control.

All data are presented as means ± SD.

Microscopic images were taken using fluorescent microscope Nikon TS100 Eclipse (Tokyo, Japan) at 100× magnification with excitation filter at 340–380 nm.

3. Results and discussion

3.1. Synthesis and spectroscopic characterization of novel probes

The synthetic route of probes **4** is illustrated in Scheme 1. Firstly, compounds **2a-2b** were achieved by nitration of xanthone [54]. Then, compounds **3a-3b** were synthesized by reduction of the nitro groups to amino moieties [54]. Finally, probes **4a-4b** were obtained by a two stage synthesis. The amines **3a-3b** were reacted with maleic anhydride in chloroform and subsequently with sodium acetate and acetic anhydride yielding **4a-4b**. The progress of the reaction was controlled by TLC chromatography. The crude probes **4a-4b** were purified by column chromatography. The purity was checked by HPLC. All compounds were synthesized in acceptable yields (52–72%). The chemical structures were confirmed with ^{1}H NMR spectroscopy and APCI mass spectrometry. The chemical shifts, multiplicities and integration of the relevant groups of protons are in accordance with the structure of the molecules. The corresponding ^{1}H NMR spectra and APCI mass spectra are shown in the Supplementary Information (Figs. S1–S4). It is worth emphasizing that the presented method of xanthone derivatives synthesis is simple and the obtained compounds can be easily purified using standard laboratory techniques.

To the best of our knowledge, the probes **4a-4b** are so far not known.

The absorption and emission properties of xanthone (**1**), the obtained probes **4a-4b** and their strongly fluorescent precursors **3a-3b** were studied by means of UV-VIS and luminescence spectroscopy in acetonitrile (MeCN) and in chloroform ($CHCl_3$) solutions. The obtained data are summarized in Tables 1. In addition, the absorption spectra of the studied compounds in MeCN are presented in Fig. 1. Excitation-emission matrix contour plots for **3a** and **3b** in MeCN are presented in Fig. 2. The derivatives **4a-4b** exhibit one absorption band in the UV region located at 341–348 nm. Whereas, the fluorescent intermediate

Table 1
The spectroscopic data of compounds **3** and **4** in different media.

	1	3a	3b	4a	4b
λ_{abs}[a], nm	339	388	410 351	341	342
ε[a], M^{-1} cm^{-1}	6200	6000	9400 8000	5900	6400
λ_{em}[a], nm	–	515	506	–	–
Stokes shift[a], nm	–	127	96	–	–
Φ_{em}[a], %	–	40	34	0.05	0.13
τ[a], ns	–	13.2	11.2	–	–
λ_{abs}[b], nm	342	381	404 346	343	343
ε[b], M^{-1} cm^{-1}	9600	6700	6900 5300	7200	5600
λ_{em}[b], nm	–	526	520	–	–
Stokes shift[b], nm	–	145	116	–	–
Φ_{em}[b], %	–	46	45	–	–
λ_{abs}[c], nm	–	–	–	345	348
ε[c], M^{-1} cm^{-1}	–	–	–	6100	6000

[a] MeCN.
[b] $CHCl_3$.
[c] H_2O (with 2% MeCN, pH 7.4).

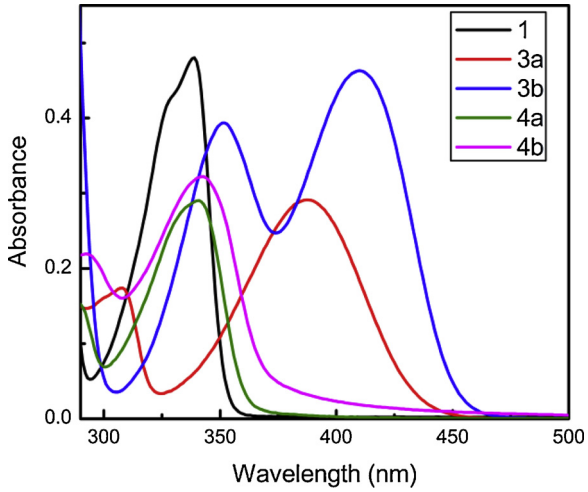

Fig. 1. Electronic absorption spectra of xanthone (**1**), compounds **3a-3b** and **4a-4b** in MeCN (50 μM).

3a exhibits one absorption band (λ_{max} = 381–388 nm) and the absorption spectra of compound **3b** shows two bands, with one band each located in both the ultraviolet and visible ranges (λ_{max} = 349–351 and 404–410 nm). The results indicate that the introduction of $-NH_2$ groups leads to a red shift in the absorption band compared with 9*H*-xanthen-9-one (**1**), which is in accordance with the electronic effects that substituents can exert. Then, the presence of maleimide groups does not cause any significant change in the absorption spectra.

2-aminoxanthone (**3a**) and 2,7-diaminoxanthone (**3b**) exhibit a fluorescence emission band with the maximum located in the range 506–526 nm. The presence of additional amino group in the structure of dye **3b** causes a small blue shift of λ_{em} in comparison with the dye **3a**. The obtained results illustrate that dyes **3a-3b** exhibit fluorescence with an emission band characterized by a Stokes shift of ˜96 to 145 nm. These values indicate that the geometries of the singlet excited states differ from the geometries of the ground states. As can be seen from data presented in Table 1, the fluorescence quantum yields (Φ_{em}) of compounds **3a-3b** ranges from 34% to 46%. The obtained fluorescence intensity decays were fitted by monexponential model (Fig. S5). The singlet lifetimes of **3a** and **3b** in MeCN are 13.2 ns and 11.2 ns, respectively.

The replacement of amino group in compounds **3a-3b** by a maleimde moiety (**4a-4b**) causes a fluorescence quenching. The fluorescence reduction by attachment of the maleimide ring proceeds *via* a photoinduced electron transfer (PET) mechanism [67]. The transfer of an electron from the excited state of fluorophore to the LUMO of the maleimide group results in decreased fluorescence due to non-radiative relaxation. After the thiol addition to the double bond in maleimide

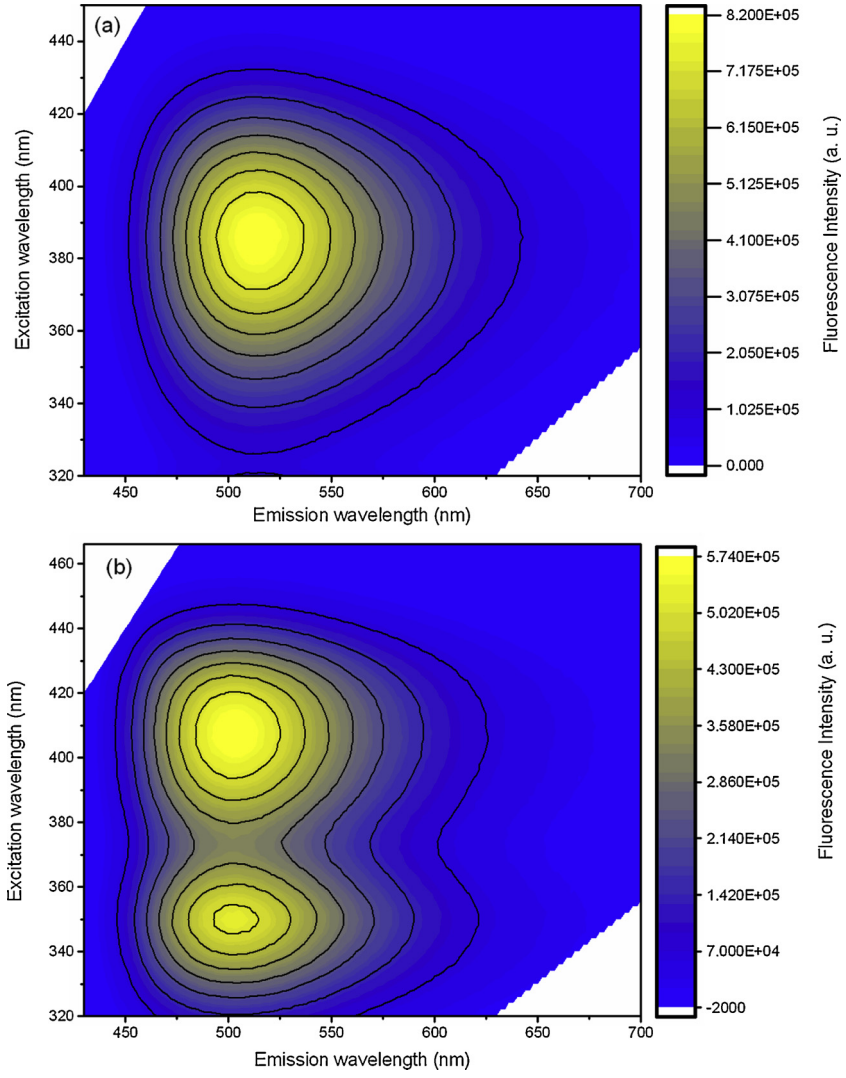

Fig. 2. Excitation-emission matrix contour plots for **3a** (a) and **3b** (b) in MeCN (20 μM).

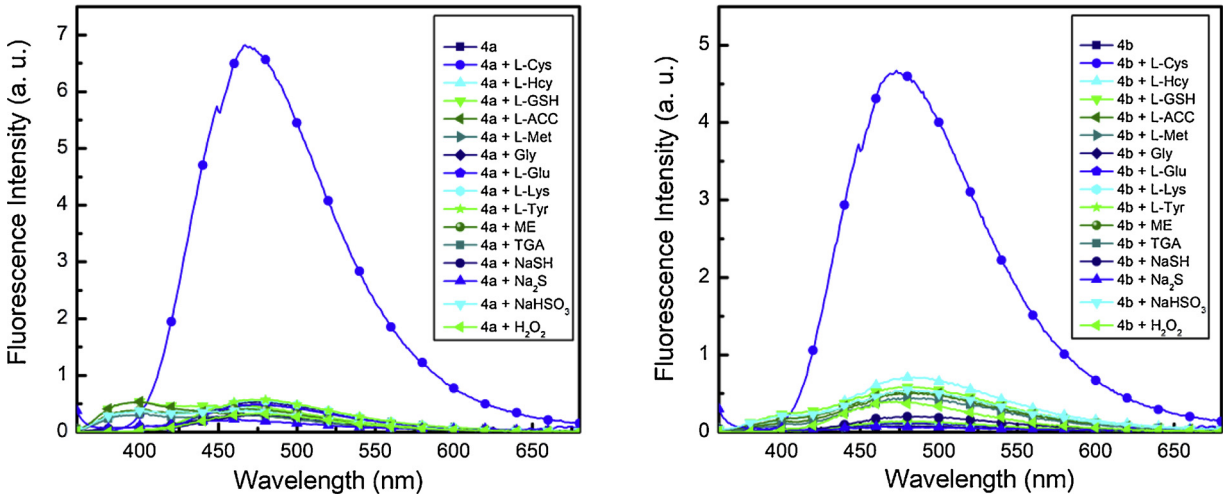

Fig. 3. The fluorescence spectra of aqueous solutions of 20 μM **4a**-**4b**, 0.1 M phosphate buffer (pH 7.4) and 2% MeCN obtained after the addition of 40 μM various analytes and the incubation at 25 °C for 15 min (λ_{ex} = 355 nm).

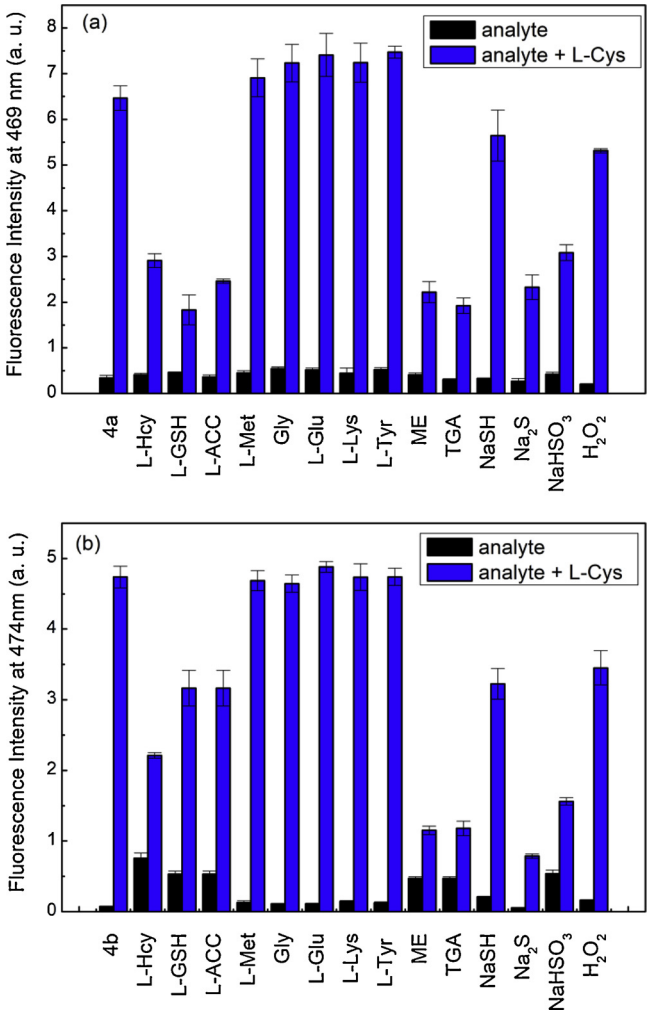

Fig. 4. The fluorescence intensity measured at λ_{em} for the solutions of 20 μM **4a**-**4b**, 0.1 M phosphate buffer (pH 7.4) and 2% MeCN without and in the presence of 40 μM various analytes and upon the addition of additional 40 μM L-Cys. The mixtures were incubated at 25 °C for 15 min (λ_{ex} = 355 nm).

moiety, the LUMO of the resulting succinimide group is higher in energy and the electron transfer from the fluorophore excited state is not thermodynamically favored. Thus, relaxation occurs directly to the ground state and the fluorescence is restored [68,69].

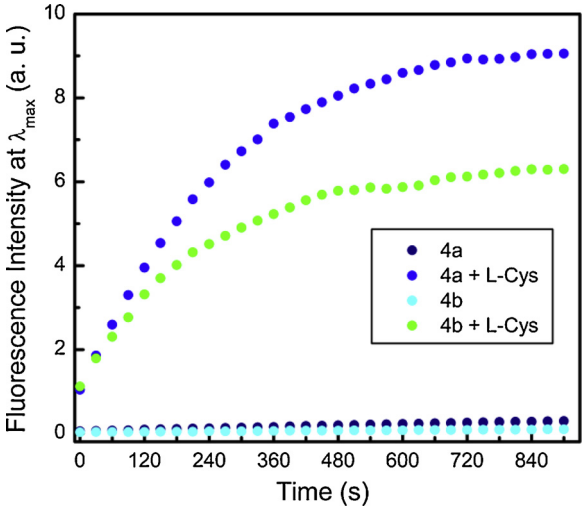

Fig. 5. Time-dependent fluorescence intensity of probes **4a**-**4b** (20 μM) without and in the presence of L-Cys (40 μM) in phosphate buffer (2% MeCN, pH 7.4). The mixtures were incubated at 25 °C for 15 min (λ_{ex} = 355 nm).

It is evident that the solvent polarity has little influence on the spectroscopic properties of the tested compounds. Despite different solvent polarity, the position of maximum absorption band was practically the same. Thus, the solvatochromism was not observed.

3.2. Studies of the fluorescent response to thiols

Regarding the application of compounds **4a**-**4b** as probes for thiols, their spectroscopic properties upon the addition different analytes were investigated.

It is obvious that the selectivity is crucial property of probes from an application point of view. To determinate the selectivity of obtained probes, the fluorescence spectra of compounds **4a**-**4b** in aqueous solutions (containing 2% MeCN as a cosolvent) in the presence of various analytes were measured. Fig. 3 illustrates the fluorescence spectra of **4a**-**4b** in the presence of different amino acids and other competitive compounds. Additionally, fluorescence intensities of tested probes at λ_{em} upon the addition of L-Cys in the presence of competitive compounds are shown in Fig. 4. The products formed upon reaction of **4a** and **4b** have intensive fluorescence with a single emission peaks at 469 nm and 474 nm, respectively. It can be seen that the addition of L-

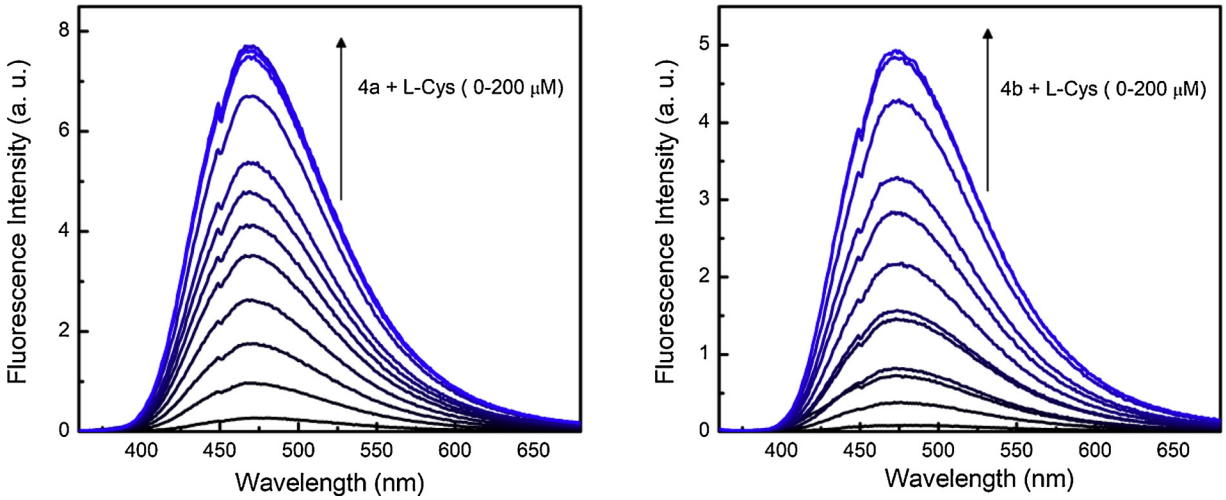

Fig. 6. The fluorescence spectra of aqueous solutions of 20 μM **4a**-**4b**, 0.1 M phosphate buffer (pH 7.4) and 2% MeCN obtained after addition of 0–200 μM L-Cys. The mixtures were incubated at 25 °C for 15 min (λ_{ex} = 355 nm).

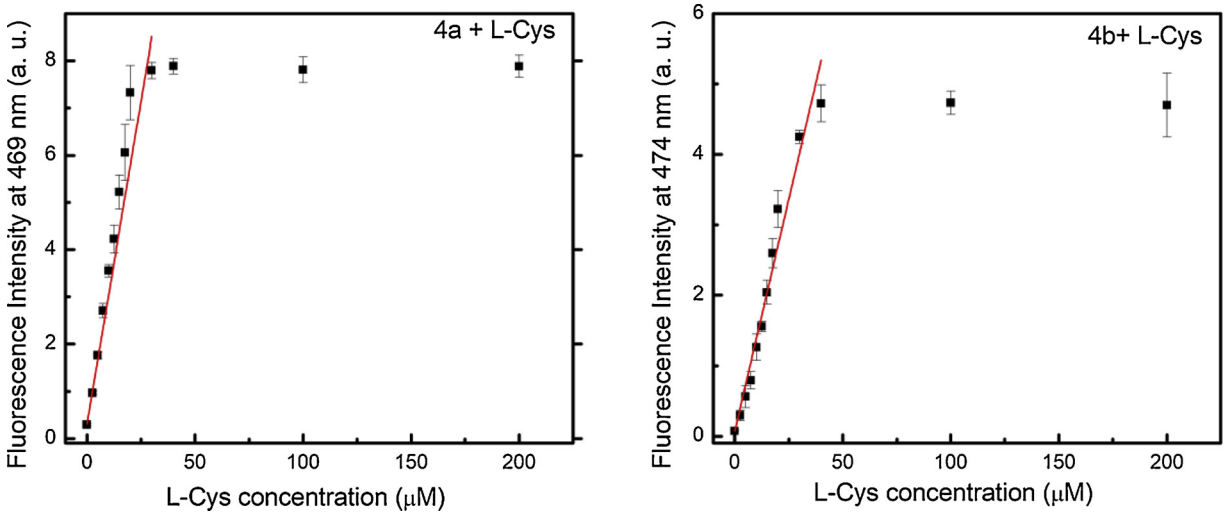

Fig. 7. The fluorescence intensity measured at λ_{em} for the solutions of 20 μM **4a**-**4b**, 0.1 M phosphate buffer (pH 7.4) and 2% MeCN after the addition of 0–200 μM L-Cys. The mixtures were incubated at 25 °C for 15 min (λ_{ex} = 355 nm). Errors bars represent the standard deviations of three trials.

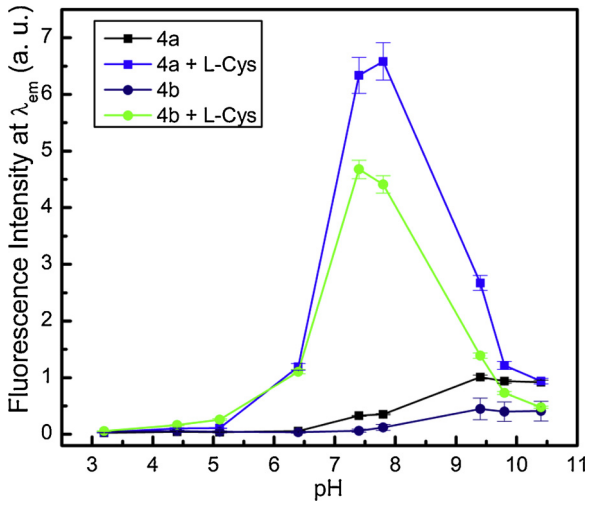

Fig. 8. The dependence of the fluorescence intensity of probes **4a**-**4b** (20 μM) at λ_{em} in the absence and in the presence of L-Cys (40 μM) on the pH values. The mixtures were incubated at 25 °C for 15 min (λ_{ex} = 355 nm).

Cys to solution of compounds **4a**-**4b** at a pH of 7.4 results in great increase of their fluorescence intensity – over 25-fold in case of **4a** and over 60-fold in case of **4b**. Moreover, the addition of other competitive analytes does not affect the fluorescence response to L-Cys and the probes selectively recognize L-Cys. However, the addition of L-Cys to solutions of probe **4a** and mercapto amino acids (L-Hcy, L-GSH and L-ACC) causes a smaller increase in fluorescent intensity than in case of the similar samples with **4b**.

The results show that no significant changes were observed in the absorption spectrum upon the addition different analytes (Figs. S6–S7). The addition of L-Cys to solution of **4a**-**4b** resulted in a small batochromic shift of their λ_{max} at a pH of 7.4.

Additionally, the time-dependent fluorescence intensity changes of compounds **4a**-**4b** in the presence of L-Cys were studied (Fig. 5). It is obvious that the addition of L-Cys to solutions of **4a**-**4b** resulted in an increase in fluorescence intensity at λ_{max} over time. In the presence of 40 μM L-Cys, the increase in fluorescence intensity of **4a**-**4b** reaches a plateau within 600 s. Thus, the fluorescence response of the tested compounds to L-Cys was obtained in a short period of time.

The response sensitivity of probes **4a**-**4b** to L-Cys was investigated by fluorescence titration experiments in aqueous solutions (containing 2% MeCN as a cosolvent, pH 7.4). Fig. 6 displays the fluorescence

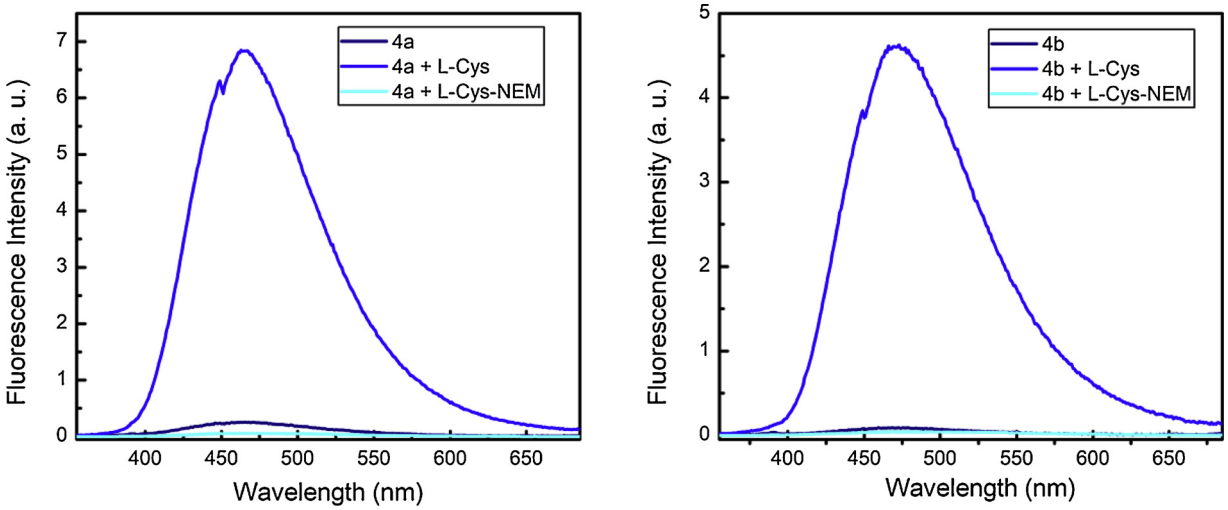

Fig. 9. The fluorescence spectra of **4a** (20 μM) and **4b** (20 μM) in the absence and in the presence of L-Cys (3 mM) and a mixture of L-Cys with NEM (3 mM) in phosphate buffer (2% MeCN, pH 7.4). The mixtures were incubated at 25 °C for 15 min (λ_{ex} = 355 nm).

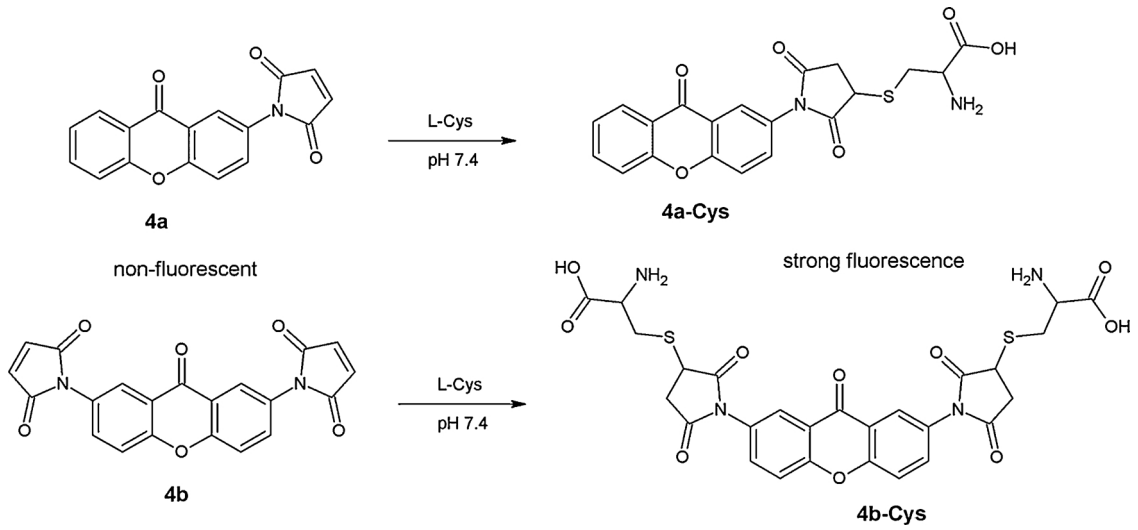

Scheme 2. The proposed reaction of studied compounds **4a**-**4b** with L-Cys.

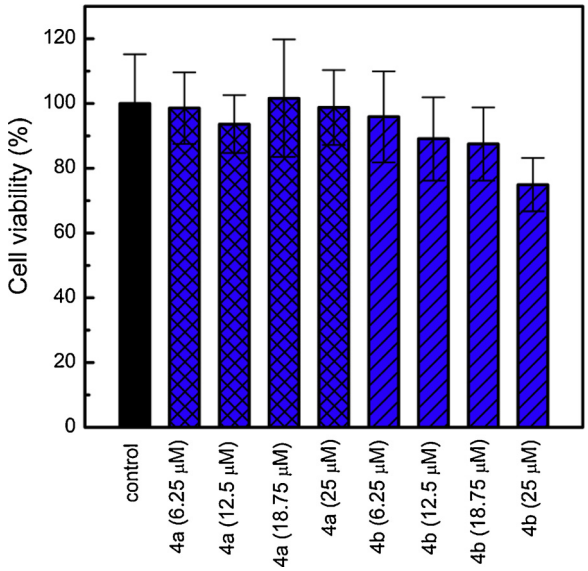

Fig. 10. The viability of the HeLa cells after treatment with compounds **4a**-**4b** for 24 h (determined using an MTT-based assay).

responses of tested probes toward different concentration of L-Cys. As shown, the fluorescence intensities at 469 nm (**4a**) and 474 nm (**4b**) increase gradually with increasing concentration of L-Cys (0–200 μM). When L-Cys concentration was in the range of 0–20 μM, the fluorescence intensity of **4a** was linearly proportional to thiol concentration, while **4b** kept a linear relationship with L-Cys concentration in the range of 0–40 μM (Fig. 7). It should be emphasized that the increase of the measured fluorescence intensity at λ_{em} was linear up to approximately 1:1 maleimide-thiol ratio, while further addition of L-Cys did not cause additional increase of the product fluorescent intensity or its decay. The reactions of **4a** and **4b** with L-Cys occur in a stoichiometric manner.

Based on these studies, the detection limits of probes for L-Cys were determined on the basis of the standard deviation of the response and the slope [70]. The detection limits were calculated according to the Eq. (3):

$$DL = \frac{3.3\sigma}{s} \quad (3)$$

where σ is the standard deviation of the response and s is the slope of the calibration curve. The estimate of σ was carried out based on the standard deviation of the blank. The fluorescence spectra of dyes without L-Cys were measured 11 times and the standard deviation of the

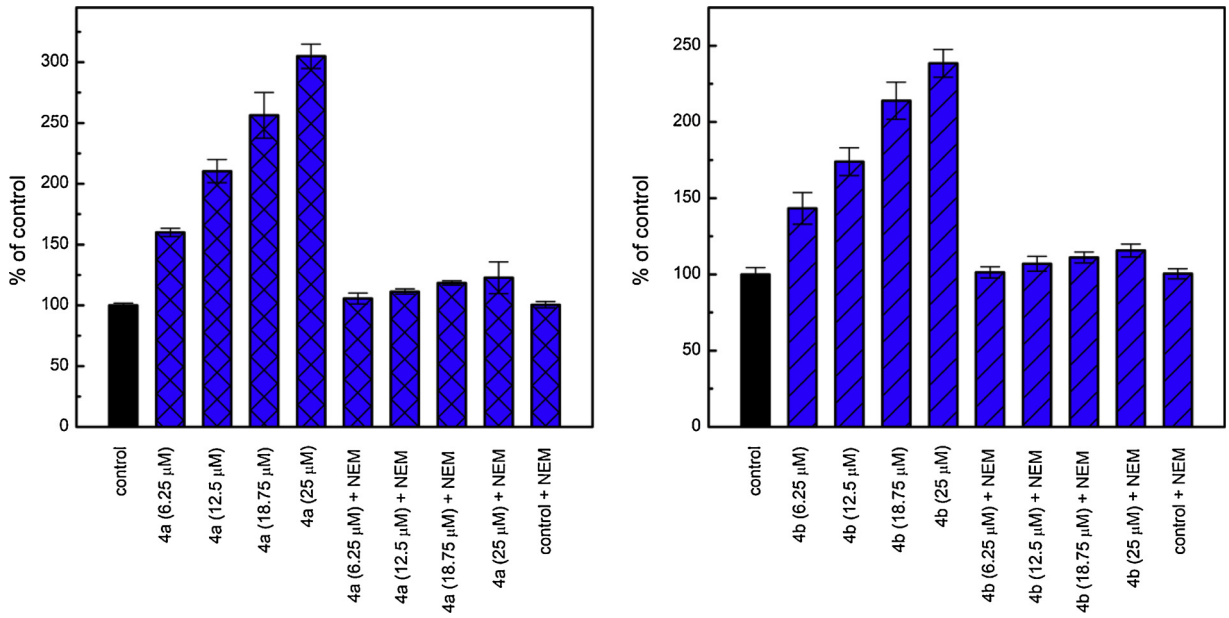

Fig. 11. Fluorescence response of compounds **4a**-**4b** (0–25 μM) in the human cells HeLa (10,000 cells per 100 μl; the fluorescence intensity at 460/40 nm was measured – λ_{ex} = 360/40 nm).

blank measurements was determined. s was obtained from plot of function fluorescence intensity of probe and L-Cys concentration.

The lowest concentration of L-Cys that can be detected by the presented fluorescent probes is 0.117 μM for **4a** and 0.121 μM for **4b**.

It is evident that, the fluorescent probes may be influenced by the pH of the extracellular and intracellular milieu. Therefore, the effect of pH on the fluorescent response of probes **4a**-**4b** to L-Cys was investigated. Fig. 8 shows the variation in fluorescence intensity for tested probes with and without L-Cys as a function of pH (3.2–10.4). In the presence of L-Cys, fluorescence intensity increased in the pH range above 5.1 to 9.4, but the highest increase in fluorescence intensity in the presence of this amino acid was observed at a physiological pH value (7.4). In the case of compounds **4a**-**4b** without L-Cys, the fluorescence intensity remains almost unchanged in the same pH range. A slight increase fluorescence intensity of **4a**-**4b** above pH 8.0 was observed. The specific behavior under more alkaline condition results from the hydrolysis process in which N-substituted maleimides are involved [28]. It can be seen from the obtained data that the investigated compounds **4a**-**4b** exhibit strong fluorescent response to L-Cys at physiological pH values.

Furthermore, the emission spectra of probes **4a**-**4b** were recorded in the presence L-Cys which was previously treated with N–ethylmaleimide (NEM – commonly used as thiol-blocking reagent) [71]. As shown in Fig. 9, L-Cys treated with NEM did not enhance the fluorescence of the studied compounds **4a**-**4b**. This suggests that the optical response toward L-Cys is the result of the reaction of the probes with sulfhydryl group present in the structure of amino acid.

It is well known from the literature that thiols are capable of addition to the double bonds of unsaturated compounds to give various of sulphides [72]. Typically, reactions involving nucleophilic addition of thiol undergo through nucleophilic attack by their thiolate anion, Thus, based on previously reported studies of the reaction mechanism between thiols and various maleimide derivatives [68,73–76], during the reaction of probes **4a**-**4b** and L-cysteine the products of the addition to the double bonds in maleimide moiety are expected to be formed. The proposed reactions between L-Cys and the obtained probes are shown in Scheme 2. Moreover, an attempt was made to confirm the mechanism of this reaction in the case of probes **4a**-**4b**. The ^{1}H NMR spectroscopic analysis provides evidence for the addition of the thiol to the double bond in maleimide moiety (Figs. S8 and S9). Upon addition of L-Cys to the DMSO-d_6 solution of probe **4a**, the signal from the protons (CH meleimide ring) at 7.08 ppm disappeared while new peaks at 4.26 ppm and in the range of 2.50–3.00 ppm were observed. A similar relationship was observed for probe **4b**. In the presence of L-Cys, the signal at 7.61 ppm disappeared and new peaks at 4.26 ppm and in the range of 2.50–3.00 ppm appeared.

Finally, a cell culture study was used to evaluate the applicability of compounds **4a**-**4b** for the detection of thiols in biological environment.

To quantify the cytotoxicity of the tested compounds **4a**-**4b,** an MTT-based assay that measured the metabolic activity of viable cells, was used. The human cell line HeLa was treated with various concentrations (0–25 μM) of the studied compounds. It was found that, upon exposure to compounds **4a**-**4b** for 24 h the majority of HeLa cells remained viable (Fig. 10).

The addition of probes **4a**-**4b** to HeLa cells resulted in an increase in fluorescence intensity at 460/40 nm (λ_{ex} = 360/40 nm) (Fig. 11). Moreover, the increase in fluorescence was linearly proportional to **4a**-**4b** concentration (Figs. S10 and S11). In the wells where the cells were pretreated with NEM and then incubated with the compounds **4a**-**4b** significant changes in fluorescence were not observed. The response was similar to the untreated control cells.

The results presented in Fig. 11 confirmed that an increase in fluorescence was caused by the reactions of the probes with thiols from HeLa cell line milieu.

Additionally, the living cell imaging experiments were performed. HeLa cells incubated with **4a**-**4b** (25 μM) in culture media for 30 min show blue fluorescence (Fig. 12D and H). The cells which were pretreated with NEM and the further incubated with **4a**-**4b** in culture media for 30 min showed non-fluorescence (Fig. 12F and J).

The obtained data demonstrated the studied probes **4a**-**4b** can be potentially used in living cell measurements.

4. Conclusions

The presented research has been focused on the synthesis of novel fluorescent probes based on a xanthone skeleton. The compounds were characterized by ^{1}H NMR spectroscopy APCI mass spectrometry. Spectroscopic studies of the presented xanthone derivatives under various conditions clearly indicates that the tested compounds are good candidates for potential application as “turn on” fluorescent probes for

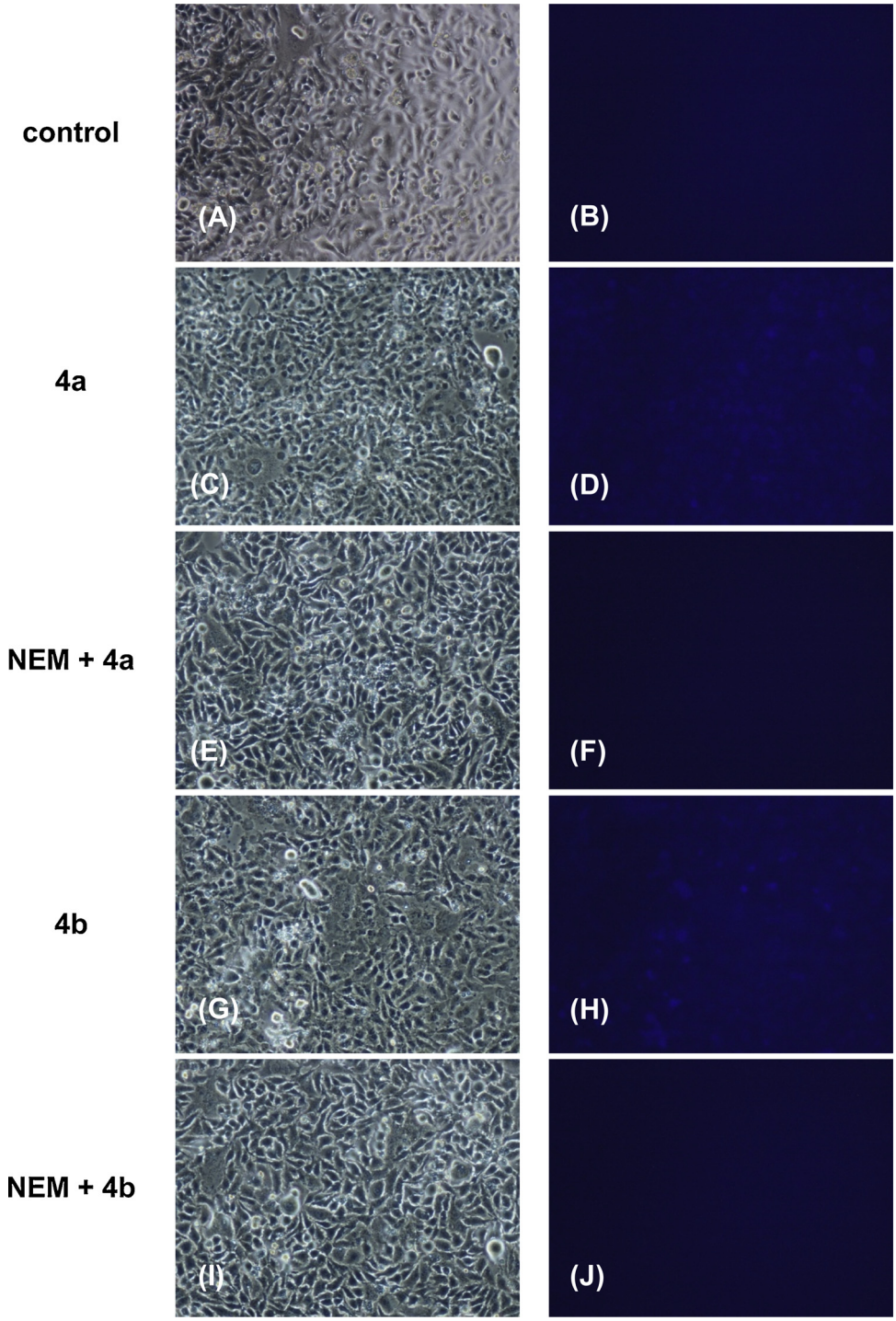

Fig. 12. Images of the HeLa cells: (A) bright-field and (B) fluorescence microscopic images of HeLa cells (control); (C, G) bright-field and (D, H) fluorescence microscopic images of HeLa cells after incubated with probes **4a**-**4b** (25 μM) for 30 min; (E, I) bright-field and (F, J) fluorescence microscopic images of HeLa cells pretreated with NEM (400 μM) for 30 min and then incubated with probes **4a**-**4b** (25 μM) for 30 min.

the detection of sulphydryl compounds, especially L-cysteine. Reaction of 2-maleimidoxanthone (**4a)** and 2,7-dimaleimidoxanthone (**4b)** with L-Cys leads to the formation of the fluorescent products under physiological conditions (pH 7.4). Fluorescence intensities of probes **4a** and **4b** have greatly enhanced 25-fold and 60-fold, respectively. The reactions of **4a** and **4b** with L-Cys occur in a stoichiometric manner and the lowest concentration of L-Cys that can be determined by the presented probes is 0.117–0.121 μM. As a proof of the concept of the usefulness of the probes **4a**-**4b** for the detection of thiols in cellular milieu, the fluorescent response of these compounds to thiols in HeLa cell line was investigated. The incubation of HeLa cells with the probes **4a**-**4b** resulted in the increase fluorescence, which was inhibited by *N*-ethylmaleimide. The presented novel derivatives of xanthone have potential application as fluorescent probes for L-Cys and can be an alternative to commonly used N-substituted maleimides.

Declaration of Competing Interest

The authors declare that they have no known competing financial interests or personal relationships that could have appeared to

influence the work reported in this paper.

Appendix A. Supplementary data

Supplementary material related to this article can be found, in the online version, at doi:https://doi.org/10.1016/j.jphotochem.2019.112153.

References

[1] A. Pompella, A. Viscikis, A. Paolicchi, V. De Tata, A.F. Casini, The changing faces of glutathione, a cellular protagonist, Biochem. Pharmacol. 66 (2003) 1499–1503, https://doi.org/10.1016/S0006-2952(03)00504-5.

[2] Y. Xiong, J.D. Uys, K.D. Tew, D.M. Townsend, S-glutathionylation: from molelecular mechanisms to health outcomes, Antioxid. Redox Signal. 15 (2011) 233–270, https://doi.org/10.1089/ars.2010.3540.

[3] T. Toyo'oka, Recent advances in separation and detection methods for thiol compounds in biological samples, J. Chromatogr. B 877 (2009) 3318–3330, https://doi.org/10.1016/j.jchromb.2009.03.034.

[4] X. Yang, Y. Wang, M. Zhao, W. Yang, A colorimetric and near-infrared fluorescent probe for cysteine and homocysteine detection, Spectrochim. Acta A. 212 (2019) 10–14, https://doi.org/10.1016/j.saa.2018.12.042.

[5] X. Chen, Y. Zhou, X. Peng, J. Yoon, Fluorescent and colorimetric probes for detection of thiols, Chem. Soc. Rev. 39 (2010) 2120–2135, https://doi.org/10.1039/b925092a.

[6] H. Peng, W. Chen, Y. Cheng, L. Hakuna, R. Strongin, B. Wang, Thiol reactive probes and chemosensors, Sensors 12 (2012) 15907–15956, https://doi.org/10.3390/s121115907.

[7] H.S. Jung, X. Chen, J.S. Kim, J. Yoon, Recent progress in luminescent and colorimetric chemosensors for detection of thiols, Chem. Soc. Rev. 42 (2013) 6019–6031, https://doi.org/10.1039/c3cs60024f.

[8] C. Yin, F. Huo, J. Zhang, R. Martinez-Manez, Y. Yang, H. Lv, S. Li, Thiol-addition reactions and their applications in thiol recognition, Chem. Soc. Rev. 42 (2013) 6032–6059, https://doi.org/10.1039/c3cs60055f.

[9] H. Peng, W. Chen, Burroughs, B. Wang, Recent advances in fluorescent probes for the detection of hydrogen sulfide, Curr. Org. Chem. 17 (2013) 641–653, https://doi.org/10.2174/1385272811317060007.

[10] N. Wang, M. Chen, J. Gao, X. Ji, J. He, J. Zhang, W. Zhao, A series of BODIPY-based probes for the detection of cysteine and homocysteine in living cells, Talanta 195 (2019) 281–289, https://doi.org/10.1016/j.talanta.2018.11.066.

[11] G. Yin, T. Niu, T. Yu, Y. Gan, X. Sun, P. Yin, H. Chen, Y. Zhang, H. Li, S. Yao, Simultaneous visualization of endogenous homocysteine, cysteine, glutatione, and their transformation through different fluorescence channels, Angew. Chem. Int. Ed. 58 (2019) 4557–4561, https://doi.org/10.1002/ange.201813935.

[12] J. Zhang, X. Ji, H. Ren, J. Zhou, Z. Chen, X. Dong, W. Zhao, Meso-heteroaryl BODIPY dyes as dual-responsive fluorescent probes for discrimination of Cys from Hcy and GSH, Sens. Actuators B-Chem. 260 (2018) 861–869, https://doi.org/10.1016/j.snb.2018.01.016.

[13] J. Gao, Y. Tao, J. Zhang, N. Wang, X. Ji, J. He, Y. Si, W. Zhao, Development of lysosome-targeted fluorescent probes for Cys by regulating the boron-dipyrromethene (BODIPY) molecular structure, Chem. Eur. J. 25 (2019) 11246–11256, https://doi.org/10.1002/chem.201902301.

[14] T. Liu, F. Huo, J. Li, J. Chao, Y. Zhang, C. Yin, An off-on fluorescent probe for specifically detecting cysteine and its application in bioimaging, Sens. Actuators B-Chem. 237 (2016) 127–132, https://doi.org/10.1016/j.snb.2016.06.080.

[15] X. Zeng, X. Zhang, B. Zhu, H. Jia, Y. Li, A highly selective wavelength-ratiometric and colorimetric probe for cysteine, Dyes Pigm. 94 (2012) 10–15, https://doi.org/10.1016/j.dyepig.2011.10.013.

[16] S. Chou, L. Ko, C. Yang, High performance liquid chromatography with fluorimetric detection for the determination of total homocysteine in human plasma: method and clinical applications, Anal. Chim. Acta 429 (2001) 331–336, https://doi.org/10.1016/S0003-2670(00)01296-4.

[17] A. Grzelakowska, J. Kolińska, M. Mąkiewicz, The synthesis and spectroscopic characterisation of 3-formyl-2-quinolones in the presence of biothiols, Color. Technol. 134 (2018) 440–449, https://doi.org/10.1111/cote.12355.

[18] O. Rusin, N.N.S. Luce, R.A. Agbaria, J.O. Escobedo, S. Jiang, I.M. Warner, F.B. Dawan, K. Lian, R.M. Strongin, Visual detection of cysteine and homocysteine, J. Am. Chem. Soc. 126 (2004) 438–439, https://doi.org/10.1021/ja036297t.

[19] X. Hou, Z. Li, B. Li, C. Liu, Z. Xu, An „off-on" fluorescein-based colorimetric and fluorescent probe for the detection of glutathione and cysteine over homocysteine and its application for cell imaging, Sens. Actuators B-Chem. 260 (2018) 295–302, https://doi.org/10.1016/j.snb.2018.01.013.

[20] B. Zhu, X. Zhang, H. Jia, Y. Li, S. Chen, S. Zhang, The determination of thiols based using a probe that utilizes both an absorption red-shift and fluorescence enhancement, Dyes Pigm. 96 (2010) 82–87, https://doi.org/10.1016/j.dyepig.2009.11.011.

[21] J.W. Nielsen, K.S. Jensen, R.E. Hansen, C.H. Gotfredsen, J.R. Winther, A fluorescent probe which allows highly specific thiol labeling at low pH, Anal. Biochem. 421 (2012) 115–120, https://doi.org/10.1016/j.ab.2011.11.027.

[22] H. Wang, G. Zhou, X. Chen, An iminofluoresecin-Cu^{2+} ensemble probe for selective detection of thiols, Sens. Actuators B-Chem. 176 (2013) 698–703, https://doi.org/10.1016/j.snb.2012.10.006.

[23] J. Huang, Y. Chen, J. Qi, X. Zhou, L. Niu, Z. Yan, J. Wang, G. Zhao, A dual-selective fluorescent probe for discriminating glutathione and homocysteine simultaneously, Spectrochim. Acta A. 201 (2018) 105–111, https://doi.org/10.1016/j.saa.2018.05.006.

[24] L. Tang, D. Xu, M. Tian, X. Yan, A mitochondria-targetable far-red emissive fluorescence probe for highly selective detection of cysteine with a large Stokes shift, J. Lumin. 208 (2019) 502–508, https://doi.org/10.1016/j.jlumin.2019.01.022.

[25] G. Yin, T. Niu, Y. Gan, T. Yu, P. Yin, H. Chen, Y. Zhang, H. Li, S. Yao, A multi-signal fluorescent probe with multiple binding sites for simultaneous sensing of cysteine, homocysteine, and glutathione, Angew. Chem. Int. Ed. 57 (2018) 4991–4994, https://doi.org/10.1002/ange.201800485.

[26] L.M. Hyman, K.J. Franz, Probing oxidative stress: small molecule fluorescent sensors of metal ions, reactive oxygen species, and thiols, Coord. Chem. Rev. 256 (2012) 2333–2356, https://doi.org/10.1016/j.ccr.2012.03.009.

[27] M.E. Langmuir, J.R. Yang, A.M. Moussa, R. Laura, K.A. LeCompte, New naphthopyranone based fluorescent thiol probes, Tetrahedron Lett. 36 (1995) 3989–3992, https://doi.org/10.1016/0040-4039(95)00695-9.

[28] M. Machida, M.I. Machida, Y. Kanaoka, Hydrolysis of N-substituted meleimides: stability of fluorescence thiol reagents in aqueous media, Chem. Pharm. Bull. 25 (1977) 2739–2743, https://doi.org/10.1248/cpb.25.2739.

[29] J. Li, C. Yin, Y. Zhang, J. Chao, F. Huo, A long wavelength fluorescent probe for biothiols and its application in cell imaging, Anal. Methods 8 (2016) 6748–6753, https://doi.org/10.1039/C6AY02150F.

[30] T. Liu, F. Huo, J. Li, J. Chao, Y. Zhang, C. Yin, A fast response and high sensitivity thiol fluorescent probe in living cells, Sens. Actuators B-Chem. 232 (2016) 619–624, https://doi.org/10.1016/j.snb.2016.04.014.

[31] Q. Wang, C. Ma, Y. Ma, X. Li, Y. Chen, J. Chen, Structure–activity relationships of diverse xanthones against multidrug resistant human tumor cells, Bioorg. Med. Chem. Lett. 27 (2017) 447–449, https://doi.org/10.1016/j.bmcl.2016.12.045.

[32] N. Szkaradek, D. Sypniewski, A.M. Waszkielewicz, A. Gunia-Krzyżak, A. Galilejczyk, S. Gałka, H. Marona, I. Bednarek, Synthesis and in vitro evaluation of anticancer potential of new aminoalkanol derivatives of xanthone, Anticancer Agents Med. Chem. 16 (2016) 1587–1604, https://doi.org/10.2174/1871520616666160404110323.

[33] J.J. Koh, H. Zou, D. Mukherjee, S. Lin, F. Lim, J.K. Tan, D.Z. Tan, B.L. Stocker, M.S. Timmer, H.M. Corkran, R. Lakshminarayanan, D.T.H. Tan, D. Cao, T.W. Beuerman, T. Dick, S. Liu, Amphiphilic xanthones as a potent chemical entity of antimycobacterial agents with membrane-targeting properties, Eur. J. Med. Chem. 123 (2016) 684–703, https://doi.org/10.1016/j.ejmech.2016.07.068.

[34] C. Proença, H.M.T. Albuquerque, D. Ribeiro, M. Freitas, C.M.M. Santos, A.M.S. Silva, E. Fernandes, Novel chromone and xanthone derivatives: synthesis and ROS/RNS scavenging activities, Eur. J. Med. Chem. 115 (2016) 381–392, https://doi.org/10.1016/j.ejmech.2016.03.043.

[35] K.M. Moon, C.Y. Kim, J.Y. Ma, B. Lee, Xanthone-related compounds as an anti-browing and antioxidant food additive, Food Chem. 274 (2019) 345–350, https://doi.org/10.1016/j.foodchem.2018.08.144.

[36] O. Chantarasriwong, A.T. Milcarek, T.B. Morales, A.L. Settle, C.O. Rezende Jr., B.D. Althufairi, M.A. Theodoraki, M.L. Alpaugh, E.A. Theodorakis, Synthesis, structure-activity relationship and in vitro pharmacodynamics of A-ring modified caged xanthones in a preclinical model of inflammatory breast cancer, Eur. J. Med. Chem. 168 (2019) 405–413, https://doi.org/10.1016/j.ejmech.2019.02.047.

[37] L. Yan, L. Zou, L. Ma, W.H. Chen, B. Wang, Z.L. Xu, Synthesis and pharmacological activities of xanthone derivatives as a-glucosidase inhibitors, Bioorg. Med. Chem. 14 (2006) 5683–5690, https://doi.org/10.1016/j.bmc.2006.04.014.

[38] Y. Liu, L. Ma, W.H. Chen, H. Park, Z. Ke, B. Wang, Binding mechanism and synergetic effects of xanthone derivatives as noncompetitive a-glucosidase inhibitors: a theoretical and experimental study, J. Phys. Chem. B 117 (2013) 13464–13471, https://doi.org/10.1021/jp4067235.

[39] L. Saraiva, P. Fresco, E. Pinto, E. Sousa, M. Pinto, J. Goncalves, Synthesis and in vivo modulatory activity of protein kinase C of xanthone derivatives, Bioorg. Med. Chem. 10 (2002) 3219–3227, https://doi.org/10.1016/S0968-0896(02)00169-4.

[40] P. Pacher, A. Nivorozhkin, C. Szabo, Therapeutic effects of xanthine oxidase inhibitors: renaissance half a century after the discovery of Allopurinol, Pharmacol. Rev. 58 (2006) 87–114, https://doi.org/10.1124/pr.58.1.6.

[41] M. Recanatini, A. Bisi, A. Cavalli, F. Belluti, S. Gobbi, A. Rampa, P. Valenti, M. Palzer, A. Palusczak, R.W. Hartmann, A new class of nonsteroidal aromatase inhibitors: design and synthesis of chromone and xanthone derivatives and inhibition of the P450 enzymes aromatase and 17-α-hydroxylase/C17,20-Lyase, J. Med. Chem. 44 (2001) 672–680, https://doi.org/10.1021/jm000955s.

[42] H. Hu, H. Liao, J. Zhang, W. Wu, J. Yan, Y. Yan, Q. Zhao, Y. Zou, X. Chai, S. Yu, Q. Wu, First identification of xanthone sulfonamides as potent acyl-CoA: cholesterol acyltransferase (ACAT) inhibitors, Bioorg. Med. Chem. Lett. 20 (2010) 3094–3097, https://doi.org/10.1016/j.bmcl.2010.03.101.

[43] P. Forterre, S. Gribaldo, D. Gadelle, M.C. Serre, Origin and evolution of DNA topoisomerases, Biochimie 89 (2007) 427–446, https://doi.org/10.1016/j.biochi.2006.12.009.

[44] M.M. Gottesman, Mechanism of cancer drug resistance, Annu. Rev. Med. 53 (2002) 615–627, https://doi.org/10.1146/annurev.med.53.082901.103929.

[45] A. Murata, T. Fukuzumi, S. Umemoto, K. Nakatani, Xanthone derivatives as potential inhibitors of miRNA processing by human dicer: targeting secondary structures of pre-miRNA by small molecules, Bioorg. Med. Chem. Lett. 23 (2013) 252–255, https://doi.org/10.1016/j.bmcl.2012.10.108.

[46] M.E. Sousa, M.M.M. Pinto, Synthesis of xanthones: an overview, Curr. Med. Chem. 12 (2005) 2447–2479, https://doi.org/10.2174/092986705774370736.

[47] J. Li, M. Hu, S.Q. Yao, Rapid synthesis, screening, and identification of xanthone- and xanthenes-based fluorophores using click chemistry, Org. Lett. 1 (2009) 3008–3011, https://doi.org/10.1021/ol9010344.

[48] A. Katori, E. Azuma, H. Ishimura, K. Kuramochi, K. Tsubaki, Fluorescent dyes with

directly connected xanthone and xanthene units, J. Org. Chem. 80 (2015) 4603–4610, https://doi.org/10.1021/acs.joc.5b00479.
[49] K.K. Ghosh, H.H. Ha, N.Y. Kang, Y. Chandran, Y.T. Chang, Solid phase combinatorial synthesis of a xanthone library using click chemistry and its application to an embryonic stem cell probe, Chem. Commun. 47 (2011) 7488–7499, https://doi.org/10.1039/C1CC11962A.
[50] B.K. Sharma, A.M. Shaikh, R.M. Kamble, Synthesis, photophysical, electrochemical and thermal investigation of triarylamines based on 9H-xanthen-9-one: yellow-green fluorescent materials, J. Chem. Sci. 127 (2015) 2063–2071, https://doi.org/10.1007/s12039-015-0973-0.
[51] D. Karak, S. Banerjee, A. Lohar, S.K. Sahana, S.S. Mukhopadhyay, D.Das Adhikari, Xanthone based Pb^{2+} selective turn on fluorescent probe for living cell staining, Anal. Methods 5 (2013) 169–172, https://doi.org/10.1039/C2AY25935D.
[52] K. Żamojć, M. Zdrowowicz, D. Jackiewicz, D. Wyrzykowski, L. Chmurzyński, Fluorescent probes used for detection of hydrogen peroxide under biological conditions, Crit. Rev. Anal. Chem. 46 (2016) 171–200, https://doi.org/10.1080/10408347.2015.1014085.
[53] S. Umemoto, J. Zhang, C. Dohno, K. Nakatani, Fluorescent ligand as a molecular probe for the RNA structure, Nucleic Acids Symp. Ser. (Oxf) 52 (2008) 211–212, https://doi.org/10.1093/nass/nrn107.
[54] T.C.S. Pace, S.L. Monahan, A.I. MacRae, M. Kaila, C. Bohne, Photophysics of aminoxanthone derivatives and their applications as binding probes for DNA, Photochem. Photobiol. 82 (2006) 78–87, https://doi.org/10.1562/2005-05-16-RA-529.
[55] M.K. Schwaebe, T.J. Moran, J.P. Whitten, Total synthesis of psorospermin, Tetrahedron Lett. 46 (2005) 827–829, https://doi.org/10.1016/j.tetlet.2004.12.006.
[56] T. Bo, H. Liu, Separation methods for pharmacolically active xanthones, J. Chromatogr. B 812 (2004) 165–174, https://doi.org/10.1016/j.jchromb.2004.08.009.
[57] Y. Na, Recent cancer drug development with xanthone structures, J. Pharm. Pharmacol. 61 (2009) 707–712, https://doi.org/10.1211/jpp.61.06.0002.
[58] I.A. Shagufta, Recent insight into the biological activities of synthetic xanthone derivatives, Eur. J. Med. Chem. 116 (2016) 267–280, https://doi.org/10.1016/j.ejmech.2016.03.058.
[59] A. Kowalska, J. Kolińska, R. Podsiadły, J. Sokołowska, Dyes derived from 3–formyl–2(1H)–quinolone – synthesis, spectroscopic characterisation, and their behaviour in the presence of sulfhydryl and non–sulfhydryl amino acids, Color. Technol. 131 (2015) 157–164, https://doi.org/10.1111/cote.12140.
[60] A. Grzelakowska, J. Kolińska, J. Sokołowska, Synthesis, spectroscopic characterisation, and potential application of dyes containing a carbostyril skeleton as sensors for thiols, Color. Technol. 132 (2016) 121–129, https://doi.org/10.1111/cote.12187.
[61] A. Grzelakowska, J. Kolińska, M. Zakłos-Szyda, R. Michalski, J. Sokołowska, Dyes derived from benzo[*a*]phenoxazine – synthesis, spectroscopic properties, and potential application as sensors for L-cysteine, Color. Technol. 133 (2017) 145–157, https://doi.org/10.1111/cote.12261.
[62] J. Kolińska, A. Grzelakowska, J. Sokołowska, Novel 7-maleimido-2(1H)-quinolones as potential fluorescent sensors for the detection of sulphydryl groups, Color. Technol. 134 (2018) 148–155, https://doi.org/10.1111/cote.12326.
[63] A.A. Goldberg, H.A. Walker, Synthesis of diaminoxanthones, J. Chem. Soc. (1953) 1348–1357, https://doi.org/10.1039/JR9530001348.
[64] F.G. Mann, J.H. Turnbull, 162. Xanthones and thioxanthones. Part I. The synthesis of 2- and 3-dialkylaminoalkylamino-derivatives, J. Chem. Soc. (1951) 747–756, https://doi.org/10.1039/JR9510000747.
[65] R. Podsiadły, R. Strzelczyk, N-substituted quinoxalinobenzothiazine/iodonium salt systems as visible photoinitiators of hybrid polymerization, Dyes Pigm. 97 (2013) 462–468, https://doi.org/10.1016/j.dyepig.2013.01.021.
[66] D. Birth, R. Imhof, Topics in fluorescence spectroscopy, Time-Domain Fluorescence Spectroscopy Using Time-Correlated Single-Photon Counting, Plenum Press, New York, 1991, pp. 1–95.
[67] R. Bonikowski, J. Kula, A. Bujacz, A. Wajs-Bonikowska, M. Zakłos-Szyda, S. Wysocki, Hydroindene-derived chiral synthons from carotol and their cytotoxicity, Tetrahedron Asymmetry 23 (2012) 1038–1045, https://doi.org/10.1016/j.tetasy.2012.07.005.
[68] K. Caron, V. Lachapelle, J.W. Keillor, Dramatic increase of quench efficiency in “spacerless” dimaleimide fluorogens, Org. Biomol. Chem. 9 (2011) 185–197, https://doi.org/10.1039/C0OB00455C.
[69] S. Girouard, M.H. Houle, A. Grandbois, J.W. Keillor, S.W. Michnick, Synthesis and characterization of dimaleimide fluorogens designed for specific labeling of proteins, J. Am. Chem. Soc. 127 (2005) 559–566, https://doi.org/10.1021/ja045742x.
[70] International Conference on harmonisation of technical requirements for registration of pharmaceuticals for human use; ICH Harmonised tripartite guideline: Validation of analytical procedures: text and methodology; 2005, p. 1-13.
[71] D.G. Smyth, A. Nagamatsu, J.S. Fruton, Some reactions of N-ethylmaleimide, J. Amer. Chem. Soc. 82 (1960) 4600–4604, https://doi.org/10.1021/ja01502a039.
[72] I.V. Koval, Reactions of thiols, Russ. J. Org. Chem. 43 (2007) 319–346, https://doi.org/10.1134/S1070428007030013.
[73] D. Kand, A.M. Kalle, P. Talukdar, Chromenoquinoline-based thiol probes: a study on the quencher position for controlling fluorescent Off-On characteristics, Org. Biomol. Chem. 11 (2013) 1691–1701, https://doi.org/10.1039/C2OB27192C.
[74] Y. Yang, F. Huo, C. Yin, J. Chao, Y. Zhang, An ‘OFF-ON’ fluorescent proce for specially recognize on Cys and its application in bioimaging, Dyes Pigm. 114 (2015) 105–109, https://doi.org/10.1016/j.dyepig.2014.11.004.
[75] T. Liu, F. Huo, C. Yin, J. Li, J. Chao, Y. Zhang, A triphenylamine as a fluorophore and maleimide as a bonding group selective turn-on fluorescent imaging probe for thiols, Dyes Pigm. 128 (2016) 209–214, https://doi.org/10.1016/j.dyepig.2015.12.031.
[76] J. Guy, K. Caron, S. Dufresne, S.W. Michnick, W.G. Skene, J.W. Keillor, Convergent preparation and photophysical characterization of dimaleimide dansyl fluorogens: elucidation of the maleimide fluorescence quenching mechanism, J. Amer. Chem. Soc. 129 (2007) 11969–11977, https://doi.org/10.1021/ja0738125.